Biomaterials 30 (2009) 6867–6878

Contents lists available at ScienceDirect

Biomaterials

journal homepage: www.elsevier.com/locate/biomaterials

The effect of substrate stiffness on adult neural stem cell behavior

Nic D. Leipzig, Molly S. Shoichet*

Department of Chemical Engineering and Applied Chemistry, Institute of Biomaterials and Biomedical Engineering, University of Toronto, Toronto, ON M5S 3E1, Canada

ARTICLE INFO

Article history:
Received 10 June 2009
Accepted 3 September 2009
Available online 23 September 2009

Keywords:
Neural stem cells
Substrate stiffness
Hydrogel scaffolds
Chitosan
Neurons
Oligodendrocytes

ABSTRACT

Adult stem cells reside in unique niches that provide vital cues for their survival, self-renewal and differentiation. In order to better understand the contribution of substrate stiffness to neural stem/progenitor cell (NSPC) differentiation and proliferation, a photopolymerizable methacrylamide chitosan (MAC) biomaterial was developed. Photopolymerizable MAC is particularly compelling for the study of the central nervous system stem cell niche because Young's elastic modulus (E_Y) can be tuned from less than 1 kPa to greater than 30 kPa. Additionally, the numerous free amine functional groups enable inclusion of biochemical signaling molecules that, together with the mechanical environment, influence cell behavior. Herein, NSPCs proliferated on MAC substrates with Young's elastic moduli below 10 kPa and exhibited maximal proliferation on 3.5 kPa surfaces. Neuronal differentiation was favored on the softest surfaces with $E_Y < 1$ kPa as confirmed by both immunohistochemistry and qRT-PCR. Oligodendrocyte differentiation was favored on stiffer scaffolds (>7 kPa); however, myelin oligodendrocyte glycoprotein (MOG) gene expression suggested that oligodendrocyte maturation and myelination was best on <1 kPa scaffolds where more mature neurons were present. Astrocyte differentiation was only observed on <1 and 3.5 kPa surfaces and represented less than 2% of the total cell population. This work demonstrates the importance of substrate stiffness to the proliferation and differentiation of adult NSPCs and highlights the importance of mechanical properties to the success of scaffolds designed to engineer central nervous system tissue.

1. Introduction

Adult tissues harbor cells that have the potential to differentiate into multiple cell types. These multipotent cells have been termed adult or somatic stem cells [1]. Adult stem cells reside within specialized microenvironments or niches incorporating numerous cell-specific cues. These cues are immensely complex but can be broadly grouped into three primary interactions: cell–cell, cell–biochemical factor and cell–matrix. Understanding the cues present in the adult stem cell niche enables the formulation of regenerative strategies that combine biomaterial design with stem cell delivery. Tissue engineering scaffold designs must incorporate cues of the native stem cell niche in order to precisely guide cell functions such as proliferation, migration and differentiation.

Populations of stem cells have been identified in the adult central nervous system (CNS) that possess the ability to self-renew, generate identical progeny and differentiate into the primary cell types found in the CNS: neurons, oligodendrocytes and astrocytes [2–4]. These neural stem/progenitor cells (NSPCs) have been isolated from two neurogenic regions of the adult brain, the hippocampus and subventricular zone (SVZ), as well as a non-neurogenic region, the spinal cord [2–4]. Recently, adult SVZ-derived NSPCs were isolated from living human patients and demonstrated self-renewal and multipotentiality [5]. NSPCs offer an attractive means of regenerating lost or damaged CNS tissue after disease or injury; however, our current understanding of the cues that drive proliferation, lineage commitment and specification in these cells is primarily limited to biochemical factors [6–9].

Recent work has shown that the mechanical properties of the matrix impact the differentiation profile of stem cells [10]. For example, fibroblasts and epithelial cells cultured on gels of varied moduli revealed that substrate stiffness can alter ECM assembly, cell spreading and cell motility [11,12]. Although the molecular pathways are yet to be characterized, it has been specifically shown that anchorage dependent cells are responsive to the mechanical properties of their matrix [10–20]. Of particular interest to central nervous system (CNS) regeneration are studies that have examined neuronal, glial and, most recently, hippocampus-derived NSPC responses to substrate elasticity [13,16,19,20]. Native brain tissue is one of the softest tissues in the body (elastic modulus (E) = 0.5–1 kPa [21,22]) compared to skeletal muscle ($E \sim 10$ kPa [23]), cartilage ($E \sim 500$ kPa [24]) and cortical bone ($E \sim 15 \times 10^6$ kPa [25]). Additionally, the brain is made of many structures such as

* Corresponding author. Donelly CCBR Room 514, 160 College St, Toronto, ON M5S 3E1, Canada.
E-mail address: molly.shoichet@utoronto.ca (M.S. Shoichet).

0142-9612/$ – see front matter © 2009 Elsevier Ltd. All rights reserved.
doi:10.1016/j.biomaterials.2009.09.002

white and grey matter, pia mater and vasculature that have elastic moduli varying from 0.5 to 50 kPa [22,26,27]. *In vitro* studies have shown that neurons, glia and NSPCs respond best to soft substrates. Neurons prefer compliant hydrogel surfaces ($E < 1$ kPa) [13,16] whereas astrocytes prefer slightly stiffer hydrogel surfaces ($E = 9$ kPa) [19]. Similarly, hippocampus-derived NSPCs differentiate into neurons on very soft substrates yet into astrocytes on stiffer substrates [20]. The study by Saha et al. [20] established a range of substrate stiffnesses to which NSPCs respond (E 0.01–10 kPa); however, differentiation to oligodendrocytes was not explored. Moreover, NSPCs utilized for experimentation were passaged up to 30 times, inevitably altering their growth properties, growth factor dependence, cell adhesion and gene expression [28].

The primary objective of this study was to determine the optimal hydrogel elastic modulus for NSPC proliferation and differentiation into all of the primary CNS lineages: neurons, oligodendrocytes and astrocytes. To accomplish this, a photocrosslinkable methacrylamide chitosan (MAC) was developed where the concentrations of a non-toxic photoinitiator and solvent were varied to control the Young's elastic modulus (E_Y) of the resulting hydrogels. Photocrosslinkable MAC provides a system where niche cues responsible for proliferation and differentiation can be identified, incorporated and translated to future 3D studies. To encourage cell adhesion, laminin, a well-known extracellular matrix protein of the nervous system [29], was incorporated into the stem cell niche design. To ensure relevant results, low passage NSPCs were seeded as single cells on these gels and total cell number, gene expression and immunohistochemistry (IHC) were characterized over time after 0, 4 and 8 d of culture.

2. Materials and methods

2.1. Methacrylamide chitosan synthesis and hydrogel formation

MAC was synthesized as described previously [30]. To form hydrogels, freeze-dried MAC was dissolved in distilled and deionized water (Millipore Milli-RO 10 Plus and Milli-Q UF Plus system at 18 MΩ resistance; Billerica, MA, USA) at 2 wt% then autoclaved. The photoinitiator 2,2-dimethoxy-2-phenylacetophenone (DMAP; Sigma–Aldrich, St. Louis, MO, USA) was dissolved into 1-vinyl-2-pyrrolidone (NVP; Sigma–Aldrich) at 300 mg DMAP per mL NVP. DMAP/NVP was sterile filtered through a 0.2 μm filter, added to 2 wt% MAC at varied concentrations v/w (1.5–30 μl DMAP/NVP per g MAC) and mixed/deaerated (SpeedMixer DAC 150 FVZ; Hauschild Engineering, Hamm, Germany). The resulting mixture was transferred to a well plate (enough to coat a 48 or 96 well) and crosslinked with 2 min UV light (365 nm) exposure. Wells were washed in sterile PBS 4 times overnight, and then coated with laminin (5 μg/mL in neurobasal media; Invitrogen, Carlsbad, CA, USA) for 4 h.

2.2. Mechanical testing

Mechanical properties were assessed via stress–relaxation tests in uniaxial, unconfined compression using a Mach-1 micromechanical testing system (Bio-Syntech, Laval, QC, Canada). MAC hydrogels were photocrosslinked, cut into 4 mm disks using biopsy punches and allowed to equilibrate for 1 d in PBS with protease inhibitors (2 mM EDTA, 5 mM benzamidine HCl, 10 mM *N*-ethylmaleimide, 1 mM phenylmethylsulfonyl fluoride; Sigma–Aldrich) at 4 °C. Samples were exposed to a 2 g tare, and then were compressed to 10% of the tare thickness at a strain rate of 1% s^{-1}. Five samples were tested for each treatment group. After the ramp displacement, stress–relaxation continued until equilibrium was reached. A simple elastic model [31] was used to determine the E_Y for each sample that was tested based on the equilibrium stress, tare height and test height.

2.3. Scanning electron microscopy

UV crosslinked MAC hydrogels were prepared as described in Section 2.1. To prepare them for scanning electron microscopy (SEM), samples were critical point dried in ethanol then sputter coated with gold. Samples were imaged using a Philips XL30 ESEM (Phillips-FEI, Hillsboro, OR, USA) with an accelerating voltage of 20 kV and spot size of 4.0.

2.4. Quantification of total adsorbed laminin

Laminin was modified with a fluorescent tag to facilitate quantification after surface adsorption. Laminin protein was reacted with 5-(and-6)-carboxyfluorescein, succinimidyl ester (5(6)-FAM,SE; Biotium, Hayward, CA, USA) at 10 times molar excess in PBS for 2 h. The resulting FAM labeled laminin was purified by HPLC (Phenomenex BioSep-SEC-S-2000, 300 by 7.8 mm, PBS buffer at 1 mL/min; Torrance, CA, USA). The purified protein concentration was determined via absorbance measurement at 280 nm (6.15×10^5 cm^{-1} M^{-1} extinction coefficient; NanoDrop ND-1000 spectrophotometer; NanoDrop Technologies, Wilmington, DE, USA). MAC gels were photocrosslinked in 96 well plates, washed in PBS 4 times overnight, then coated with FAM–laminin for 4 h in PBS. The plates were placed in a 37 °C incubator and the PBS was fully changed at days 0, 1 d and a half volume change was performed at 4 d. The concentration of laminin adsorbed to gels was determined via fluorescent measurement (495 nm excitation, 519 nm emission; Molecular Devices SpectraMAX Gemini EM, Sunnyvale, CA, USA) and quantified by comparison to a standard curve.

2.5. Cell isolation and culture

NSPCs were isolated from the subependymal region of the lateral ventricles in the forebrain of adult female Wistar rats and expanded in neurosphere culture as explained previously [32]. NSPCs were expanded in growth medium containing neurobasal media (Invitrogen), B27 neural supplement (Invitrogen), 2 mM L-glutamine (Sigma–Aldrich), 100 μg/mL penicillin–streptomycin (Sigma–Aldrich), 20 ng/mL epidermal growth factor (EGF – recombinant human; Invitrogen), 20 ng/mL basic fibroblastic growth actor (bFGF – recombinant human bFGF; Invitrogen) and 2 μg/mL heparin (Sigma–Aldrich). The resulting neurospheres were passaged 3–4 times before experimentation. Neurospheres were dissociated into single cells by pipetting and then counted with a hemocytometer using trypan blue (Sigma–Aldrich) exclusion. Dissociated cells were plated on the surface of MAC hydrogels in growth media and incubated at 37 °C and 5% CO_2 and cultured for 18 h. The growth media was removed and replaced with differentiation medium containing neurobasal media, 2 mM L-glutamine, 100 μg/mL penicillin–streptomycin, and 1% fetal bovine serum (FBS). Cells were cultured in differentiation medium for an additional 7 d. To test the cytotoxicity response to photocrosslinked MAC, NSPCs were plated on laminin-coated glass coverslips (2 cm diameter) in a 24 well plate and allowed to attach for 4 h. Photocrosslinked hydrogels were made by adding photoinitiator/solvent (DMAP/NVP) at v/w concentrations of 1.5–30 μL per g of MAC. 0.5 mL of the resulting mixtures were added to a 48 cell plate, exposed to UV light, and then washed three times with PBS. These MAC hydrogels were placed in culture inserts (0.4 μm, BD Biosciences, Franklin Lakes, NJ, USA) and placed in the same well plate as NSPCs, forming two compartments sharing the same media. This allowed cells to be exposed to MAC scaffolds without direct contact. A control group was included with a cell culture insert and no MAC scaffold (media). Culturing was performed for 1 d in growth media followed by 7 d in differentiation media.

Table 1
Primer and probe designs for quantitative RT-PCR.

Gene[a] (Accession number, product size)	Forward primer Reverse primer
Hypoxanthine phosphoribosyltransferase 1 (HPRT; NM_012583, 123 bp)	CTCATGGACTGATTATGGACAGGAC GCAGGTCAGCAAAGAACTTATAGCC
Glyceraldehyde-3-phosphate dehydrogenase (GAPDH; NM_017008, 169 bp)	TCACCACCATGGAGAAGGC GCTAAGCAGTTGGTGGTGCA
2′,3′-Cyclic nucleotide 3′-phosphodiesterase (CNPase; NM_012809, 79 bp)	CAACAGGATGTGGTGAGGA CTGTCTTGGGTGTCACAAAG
Myelin oligodendrocyte glycoprotein (MOG; NM_022668, 92 bp)	CTCATTGCCCTTGTGCCTA GCACGGAGTTTTCCTCTCAG
Oligodendrocyte transcription factor 1 (OLIG1; NM_021770, 154 bp)	AAGGAGGACATTTCCAGACTTC GCTCTAAACAGGTGGGATTCATC
βIII tubulin (NM_139254, 96 bp)	ACTTTATCTTCGGTCAGAGTG CTCACGACATCCAGGACTGA
Neuron specific enolase 2 (NSE; NM_139325, 86 bp)	GAGAACAGCGAAGCTTTGG AGCCACATCCATACCAATCA
Doublecortin (DCX; NM_053379, 52 bp)	TGCGCCCCAAACTTGTG CGCCTTCCGAGGCTTCA
Glial fibrillary acidic protein (GFAP; NM_017009, 89 bp)	GAGAGAGATTCGCACTCAGTA TGAGGTCTGCAAACTTGGAC
S100 calcium binding protein B (S100B; NM_013191, 92 bp)	TTCCTGGAGGAAATCAAAGAG AGGCCATAAACTCCTGGAAG
Nestin NM_012987, 118 bp)	TGGCACACCTCAAGATGTCCCTTA AGAAAGCCAAGAGAAGCCTGGGAA
Paired box protein 6 (PAX6; NM_013001, 92 bp)	TCTGGAGAAAGAGTTTGAGAG GTATCCTTGCTTCAGGTAGA

[a] All sequences are 5'–3'.

2.6. Quantification of total cell number

Cells were lysed after 4 and 8 d by freeze-thaw in 1× Tris-EDTA buffer and 0.2% Triton X-100 (Sigma–Aldrich). Total double-stranded DNA was measured by fluorescence (Molecular Devices) via the reaction of DNA with PicoGreen dye (PicoGreen dsDNA Quantitation Kit; Invitrogen). 2.1 pg of DNA/cell was used to convert concentration of dsDNA to total number of cells, as was experimentally determined for rat SVZ-derived NSPCs.

2.7. Immunohistochemistry

The following primary antibodies were used for immunohistochemistry (IHC): monoclonal mouse anti-β-III tubulin (1:1000; Abcam, Cambridge, MA, USA) for neurons; monoclonal anti-RIP (1:5; Developmental Studies Hybridoma Bank, Iowa City, IA, USA) for oligodendrocytes; and monoclonal mouse anti-glial fibrillary acidic protein (GFAP, 1:100; Cell Sciences, Canton, MA, USA) for astrocytes and monoclonal mouse anti-nestin (1:500; BD Biosciences, San Jose, CA, USA). For all IHC procedures, appropriate controls were obtained by omission of the relevant primary antibody. Cells on MAC substrates were fixed after 4 and 8 d of culture with PBS solution containing 4% paraformaldehyde (Sigma–Aldrich) for 20 min at room temperature and then washed with PBS 3 times. Cell membranes were permeabilized with 0.1% Triton X-100 in PBS for 10 min, washed 3 times then blocked with a solution of 10% FBS in PBS at room temperature for 1 h. Next, each primary antibody solution was added for 24 h at 4 °C. After washing with PBS 3 times, samples were exposed to secondary goat anti-mouse IgG Alexa-Fluor 546 (1:400; Invitrogen) for 2 h at room temperature and then washed with PBS buffer 3 times. Finally, cell nuclei were counterstained with 10 μM Hoechst 33342 (Invitrogen) for 7 min, washed with PBS buffer and mounted/coverslipped using ProLong Gold anti-fade reagent (Invitrogen).

2.8. Total RNA isolation and real-time RT-PCR

Cells were lysed at days 0, 4 and 8 and total RNA was isolated using the RNAqueous micro kit (Ambion, Austin, TX, USA). Day 0 samples were obtained from the cell seeding solution. After RNA isolation, DNase I treatment was performed followed by the measurement of total RNA concentration and purity (NanoDrop ND-1000). For the reverse transcription (RT) reaction, 15.7 μL of RNA (at 5 ng total RNA/μL) was incubated with oligo(dT) primers and random hexamers at 65 °C for 5 min. After cooling to room temperature, the RNA-oligo(dT)/hexamer mix, buffer, dNTPs, RNase inhibitor, Stratagene and AffinityScript RT enzyme (La Jolla, CA, USA) was incubated for 60 min at 42 °C. The reaction was terminated by 70 °C for 15 min. Quantitative reverse transcriptase-polymerase chain reaction (qRT-PCR) amplification was performed with an Applied Biosystems 7900HT (Foster City, CA, USA) using SYBR Green I (Invitrogen) detection chemistry. The 5′–3′ sequences for the forward primers and reverse primers were designed from rat mRNA sequences from the National Center for Biotechnology Information (NCBI) and are given in Table 1. For qRT-PCR analysis of each sample, the following were prepared in a 11 μL reaction buffer: 1 μL of DNA sample, 1× buffer, 3-4 mM $MgCl_2$, 0.2 mM DNTPs, 200–400 nM of each forward and reverse primer, 0.5× SYBR Green I, 1× ROX reference dye (Sigma–Aldrich), and 0.055 U HotStarTaq (Qiagen, Valencia, CA, USA). Quantitative RT-PCR amplification was achieved with a 15 min activation step at 95 °C, followed by 50 cycles of 15 s at 94 °C, 30 s at 60 °C, 60 s at 72 °C and a fluorescence measurement. All qRT-PCR reactions were performed in triplicate. A standard curve (cycle

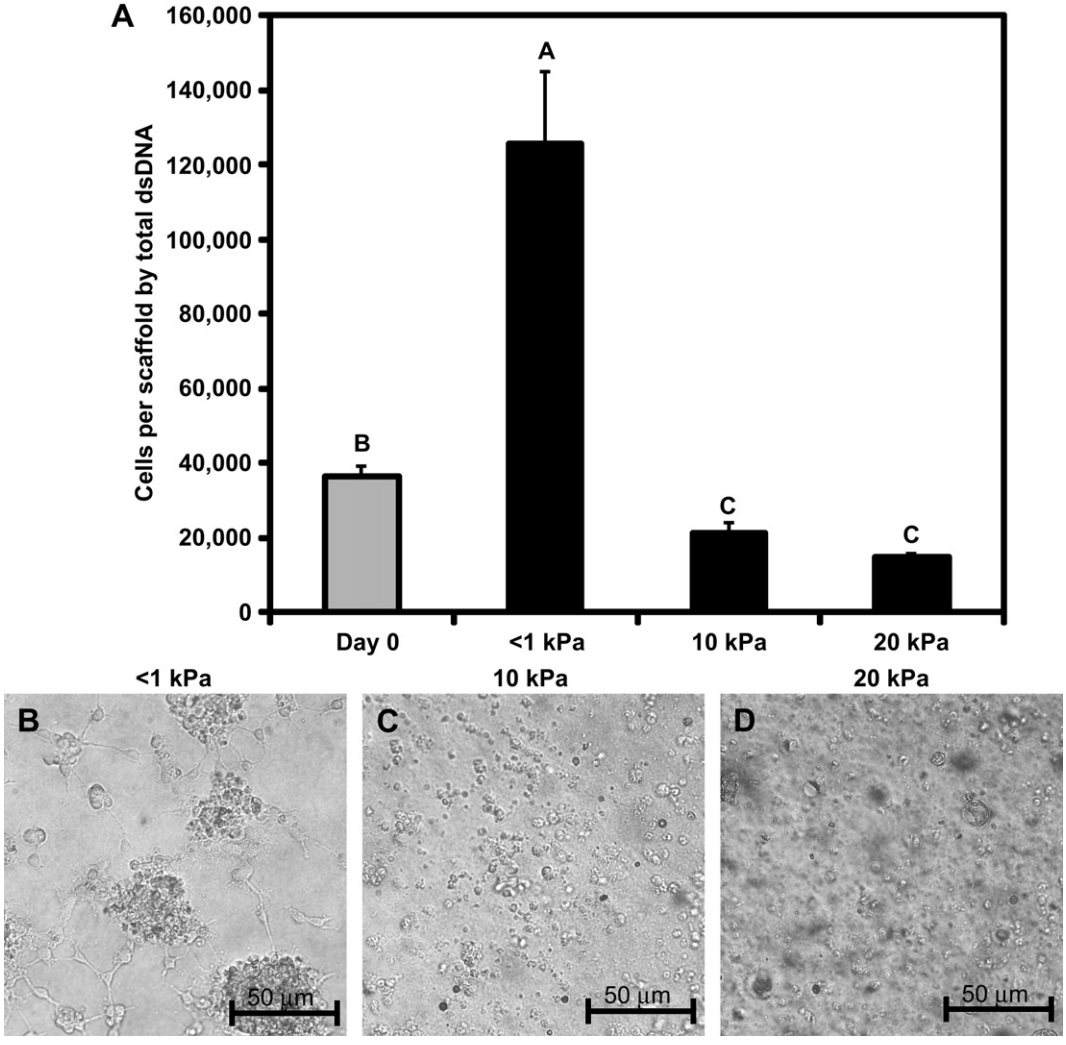

Fig. 1. (A) Total cell number by PicoGreen assay for total dsDNA and images of NSPCs seeded and differentiated on MAC hydrogels with (B) $E_Y < 1$, (C) $E_Y = 10$ kPa, (D) $E_Y = 20$ kPa after 8 d of culture. Total cell number significantly increased only on <1 kPa MAC at day 8 as compared to day 0 ($p < 0.0001$); cell number significantly decreased on both 10 kPa and 20 kPa hydrogels relative to day 0. Cell culture images show striking differences in cell number and morphology on these surfaces. Colony formation and cell processes were only observed on <1 kPa MAC. Different letters indicate significant differences by one-factor ANOVA ($p < 0.05$). Data are presented as mean ± SD, $n = 3$.

threshold value versus relative template concentration) was prepared for each target gene and for the endogenous references (HPRT and GAPDH). Gene expression for each target gene was compared to controls (day 0), and the relative fold change was calculated by normalizing against the endogenous reference genes using Pfaffl's efficiency corrected calculation model for multiple reference genes [33].

2.9. Statistical analysis

All statistical analyses were performed using JMP IN 7.1 (SAS Institute, Cary, NC, USA). Differences among groups were assessed by ANOVA with Tukey's *post hoc* analysis to identify statistical differences among three or more treatments. All data is presented as mean ± SD.

3. Results

3.1. Hydrogel properties

The concentration of DMAP in NVP was varied to control the elastic modulus of the resulting photocrosslinked methacrylamide chitosan gels. By increasing the concentration of DMAP dissolved in NVP while maintaining both the UV exposure time and the concentration of methacrylamide, a series of crosslinked methacrylamide gels were synthesized and characterized in terms of their mechanical properties and pore size distribution. Crosslinked MAC scaffolds were produced with elastic moduli ranging from <1 to 20 kPa using 1.5 to 15 μl of 300 mg/mL of DMAP/NVP and 1 g of 2 wt% MAC dissolved in water. On MAC hydrogels with $E_Y < 10$ kPa, NSPCs proliferated, formed colonies and differentiated (Fig. 1), whereas on MAC hydrogels with $E_Y \geq 10$ kPa, cells exhibited neither a proliferative response nor colony formation, differentiating primarily to oligodendrocytes (>75% of the total population) with little to no neuron and astrocyte differentiation (data not shown). Consequently, NSPCs' responses were studied on MAC scaffolds with $E_Y < 10$ kPa. Three crosslinked MAC scaffolds were synthesized using 1.5, 3.0 and 6.0 μL of 300 mg/mL DMAP/NMP with 1 g of 2 wt% MAC in water resulting in scaffolds with E_Y equal to 0.80 ± 0.18, 3.59 ± 0.51 and 6.72 ± 0.58 kPa, referred to as <1, 3.5 and 7 kPa, respectively.

The porosity of these hydrogels was examined by scanning electron microscopy. SEM images of UV-crosslinked MAC showed a porous network which varied slightly among the three Young's elastic moduli materials studied (Fig. 2A). Increasing Young's elastic modulus resulted in more crosslinks and smaller internal pores.

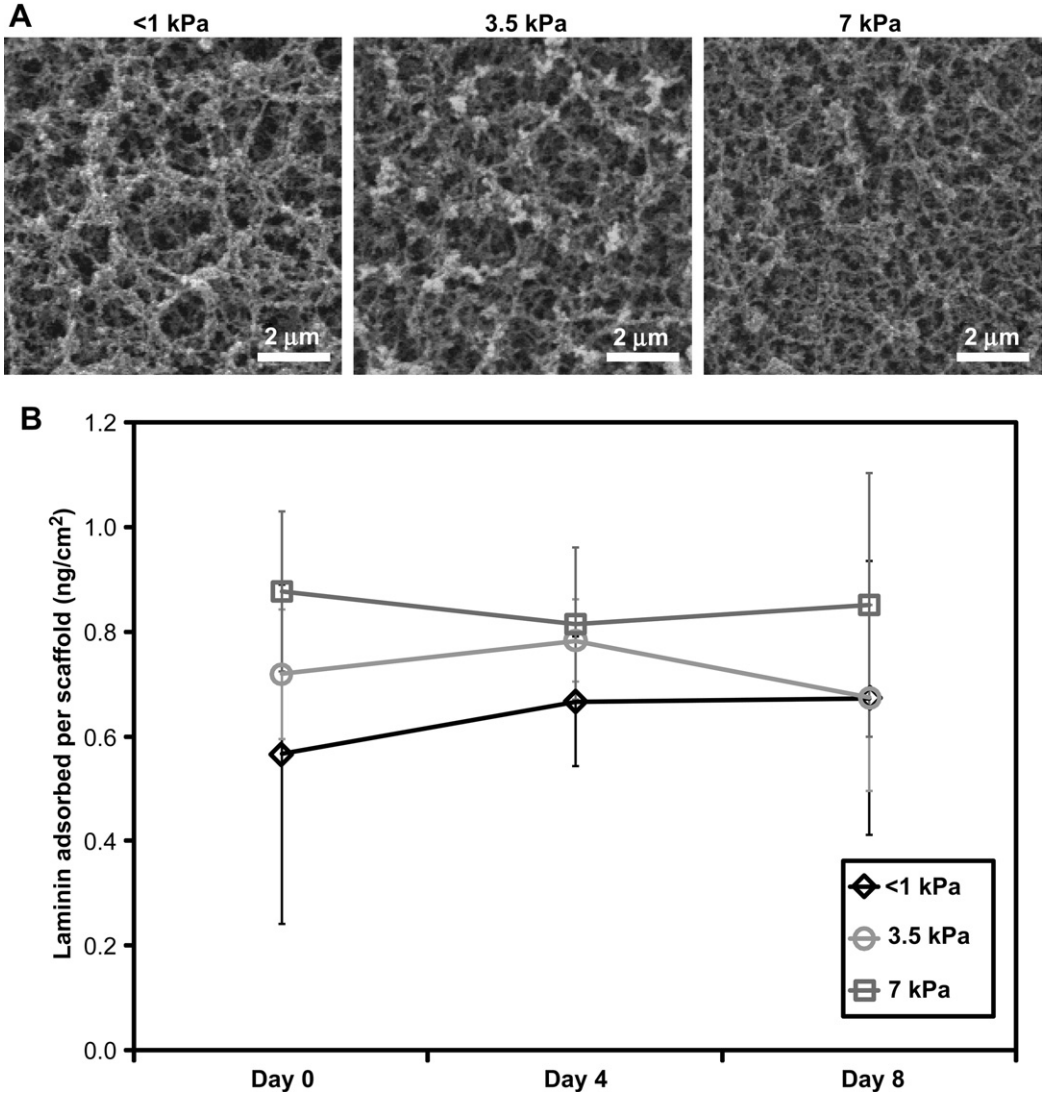

Fig. 2. (A) SEM and (B) quantification of laminin adsorbed onto MAC hydrogel surfaces. SEM of critically point dried and gold sputter coated MAC hydrogels shows that the surface is made up of a tightly crosslinked network and that the porosity decreases as E_Y increases. Fluorescently tagged (FAM)–laminin protein was adsorbed to MAC hydrogel surfaces and incubated at 37 °C with PBS changed after days 0, 1 and 4. Quantification of the amount of FAM–laminin on surfaces revealed that the concentration did not significantly vary with scaffold stiffness or time (two-factor ANOVA, $p > 0.1$). Data are presented as mean ± SD, $n = 3$.

Despite the observed differences in crosslinking density, the amount of laminin adsorbed to these three MAC surfaces was not statistically different and did not change significantly with time (Fig. 2B, $p > 0.1$); however, a trend was observed towards more laminin adsorption on stiffer MAC for all time points.

3.2. Cytocompatibility of MAC hydrogels

MAC hydrogels were shown to be compatible with NSPCs irrespective of crosslinker concentrations of DMAP/NVP between 1.5 and 30 v/w (Fig. 3). Cells proliferated in all treatment groups as evidenced by significantly higher total cell numbers relative to day 0 samples ($p < 0.0001$).

3.3. Cells cultured on MAC hydrogels

NSPCs were plated on the three MAC hydrogels with different moduli and found to adhere and form colonies on MAC gels with E_Y equal to <1, 3.5 and 7 kPa (Fig. 4). The 3.5 kPa surfaces generated the largest colonies, especially by culture day 8. Cell process extension and migration was only observed on <1 kPa MAC scaffolds, first appearing at 4 d of culture and noticeably increasing by day 8.

NSPCs proliferated on all three surfaces as measured quantitatively for total cell number during the culture period (Fig. 5). The resulting cell doubling times on <1, 3.5 and 7 kPa MAC were 139.5, 111.4 and 185.67 h, respectively. By day 8, total cell numbers on MAC surfaces were significantly higher than day 0 ($p < 0.0001$). The 3.5 kPa MAC surfaces supported the most cells at both days 4 and 8 ($p < 0.001$).

3.4. Immunohistochemistry

NSPCs primarily differentiated into oligodendrocytes on MAC surfaces. Fluorescent microscopy showed that the majority of RIP positive cells were found in colonies on the MAC surfaces (Fig. 6A) and that these cells formed interconnected networks with other RIP positive cells. The 7 kPa surfaces yielded more RIP-positive oligodendrocytes ($71.8 \pm 2.7\%$) than the less stiff surfaces where $67.5 \pm 5.6\%$ and $59.4 \pm 2.6\%$ oligodendrocytes were observed on 3.5 and <1 kPa surfaces, respectively (Fig. 6A, $p < 0.001$). The <1 kPa MAC hydrogels significantly promoted both βIII-tubulin positive neuron and GFAP positive astrocyte differentiation over the 3.5 and 7 kPa MAC surfaces (Fig. 6B,C, $p < 0.0001$). The <1 kPa MAC resulted in $32.9 \pm 2.0\%$ neurons whereas the 3.5 kPa resulted in $22.5 \pm 1.7\%$ neurons and the 7 kPa in $11.6 \pm 0.8\%$ neurons. βIII tubulin positive cells (neurons) were observed interspersed in colonies on all surfaces yet migrated out of colonies on only <1 kPa surfaces (Fig. 6B). GFAP positive cells (astrocytes) only appeared in large colonies at low frequencies ($1.9 \pm 0.4\%$ on <1 kPa and $1.0 \pm 0.3\%$ on 3.5 kPa) and were not observed on 7 kPa surfaces (Fig. 6C).

3.5. Quantitative RT-PCR

Quantitative RT-PCR analysis for oligodendrocyte markers demonstrated that <1 kPa MAC yielded the highest mRNA levels of CNPase, an early expressed mature oligodendrocyte marker, at day 8 with an 11.8 ± 1.7 fold increase over day 0 (Fig. 7A, $p < 0.0001$). Similarly, <1 kPa surfaces yielded the highest expression of the later expressed mature oligodendrocyte marker MOG with a 15.5 ± 2.6 fold increase over day 0 (Fig. 7B, $p < 0.0001$). MOG expression increased over the culture period on both <1 and 3.5 kPa MAC yet was not detectable on 7 kPa surfaces. The transcriptional marker OLIG1 was significantly upregulated on 3.5 kPa surfaces at day 4 with a 2.1 ± 0.1 fold increase relative to day 0 (Fig. 7C, $p < 0.001$). However, on day 8 OLIG1 expression on all surfaces returned to day 0 levels (Fig. 7C, $p > 0.05$).

MAC surfaces with an $E_Y < 1$ kPa yielded the highest mRNA levels for three neuronal markers: βIII tubulin, NSE, DCX. Expression of βIII tubulin, an early neuronal marker, reached the greatest levels by day 8 on <1 kPa MAC with a 2.8 ± 0.2 fold increase from day 0 (Fig. 8A, $p < 0.0001$). Messenger-RNA levels for the mature neuronal marker NSE, significantly increased by day 8 of culture for

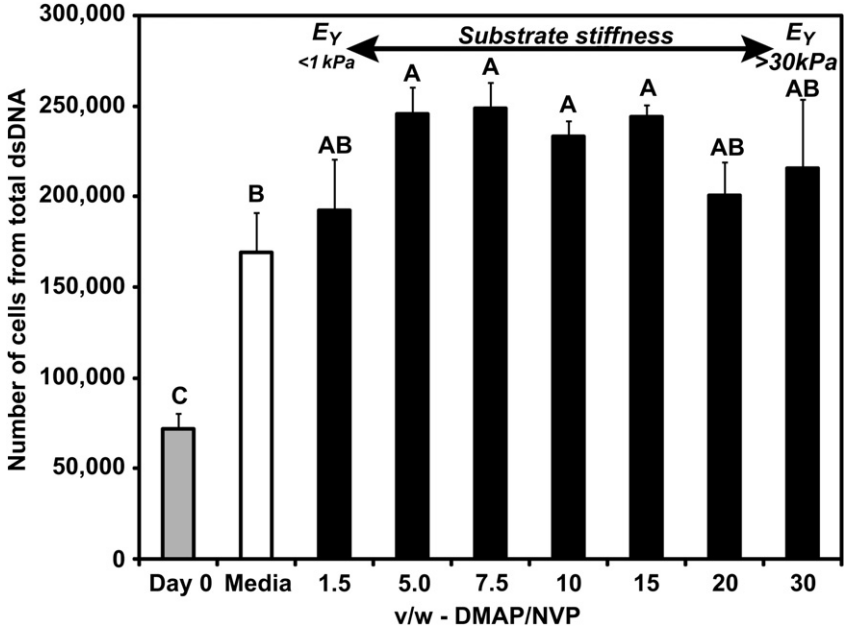

Fig. 3. Toxicity response of NSPCs to UV crosslinked MAC scaffolds after 8 d. MAC hydrogels were formed using photoinitiator/solvent (DMAP/NVP) at v/w concentrations of 0 (media only) to 30 μL per g of MAC. NSPCs were seeded onto laminin-coated glass coverslips and cultured for 8 d in wells in which MAC scaffolds had been placed in transwell inserts. Thus the NSPCs were exposed to MAC scaffolds but not in direct contact with them for the 8 d culture period. The total cell number for each treatment group demonstrated that the UV crosslinked MAC hydrogels were not cytotoxic and NSPCs proliferated in the presence of gels comprising 5.0–15 v/w DMAP/NVP as compared to media alone controls ($p < 0.0001$). Different letters indicate significant differences by one-factor ANOVA ($p < 0.05$). Data are presented as mean ± SD, $n = 3$.

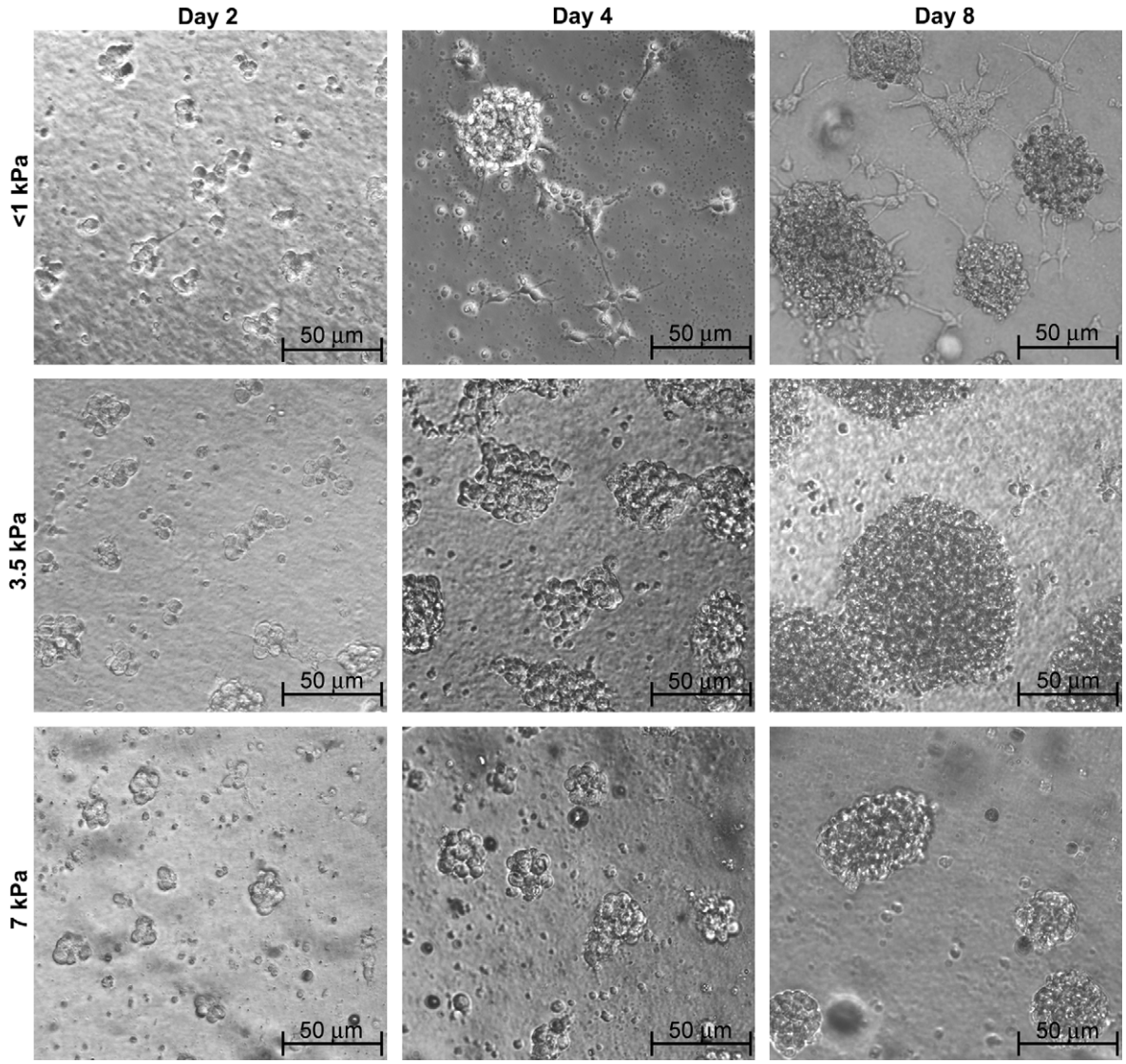

Fig. 4. Representative images of NSPCs seeded and differentiated on MAC hydrogels of varied substrate stiffness over 8 d of culture. Cells attach as single cells and proliferate on all surfaces in the form of colonies. 3.5 kPa MAC surfaces stimulated the largest colonies by day 8. Cell process formation and migration out of colonies was only observed on < 1 kPa surfaces.

<1 and 3.5 kPa scaffolds with a 4.0 ± 1.3 and 2.8 ± 1.1 fold increase, respectively, over day 0 (Fig. 8B, $p < 0.001$). Expression of the neuron migrational marker DCX at day 8 only increased on <1 kPa MAC with a 1.6 ± 0.2 fold increase over day 0 (Fig. 8C, $p < 0.001$).

Expression of the mature astrocyte markers GFAP and S100B significantly increased on <1 and 3.5 kPa MAC over the culture period. By day 8, GFAP mRNA levels reached a 70.7 ± 13.2 fold increase on <1 kPa hydrogels followed by a 28.7 ± 13.2 fold increase over day 0 on 3.5 kPa MAC surfaces (Fig. 9A, $p < 0.0001$). GFAP expression was not detected in cells cultured on 7 kPa MAC. The expression of S100B significantly increased at day 8 for <1 and 3.5 kPa scaffolds with a 4.6 ± 0.8 and 3.2 ± 0.8 fold increase, respectively, over day 0 (Fig. 9B, $p < 0.05$).

Quantitative PCR analysis revealed that expression of the progenitor markers, nestin and PAX6, decreased over 8 d of culture. Nestin mRNA levels significantly decreased for all treatments (Fig. 9C, $p < 0.05$). On <1 and 3.5 kPa surfaces, expression of PAX6, a marker tied to neuronal progenitor formation [34,35], remained the same at day 4 before down regulating expression to undetectable levels by day 8 (Fig. 9D, $p < 0.0001$).

4. Discussion

The microenvironmental stimuli necessary to guide stem cell behavior are beginning to be understood. These stimuli involve a complex combination of chemical and physical cues and are highly dependent on cell type as well as their tissue of origin. The stiffness of the matrix has been recently shown to be important to both differentiated and undifferentiated cell types derived from the nervous system [13,16,19,20]. Our primary goal was to determine how the substrate stiffness of a biomaterial scaffold influenced proliferation and differentiation of low passage SVZ-derived adult NSPCs, an adult stem cell that has demonstrated clinical relevance [5].

MAC offers a valuable platform for studying NSPC responses to substrate stiffness in mixed differentiation media conditions (1% FBS) because the elastic modulus can be easily tuned while providing a cell-adhesive environment. By controlling the amount of photoinitiator included in the UV crosslinking reaction, substrate stiffness (E_Y) was tuned to match that of CNS tissue (Fig. 3). Scaffolds with compressive E_Y ranging from <1 kPa to 30 kPa were easily created from solutions containing equal weight percentages of MAC

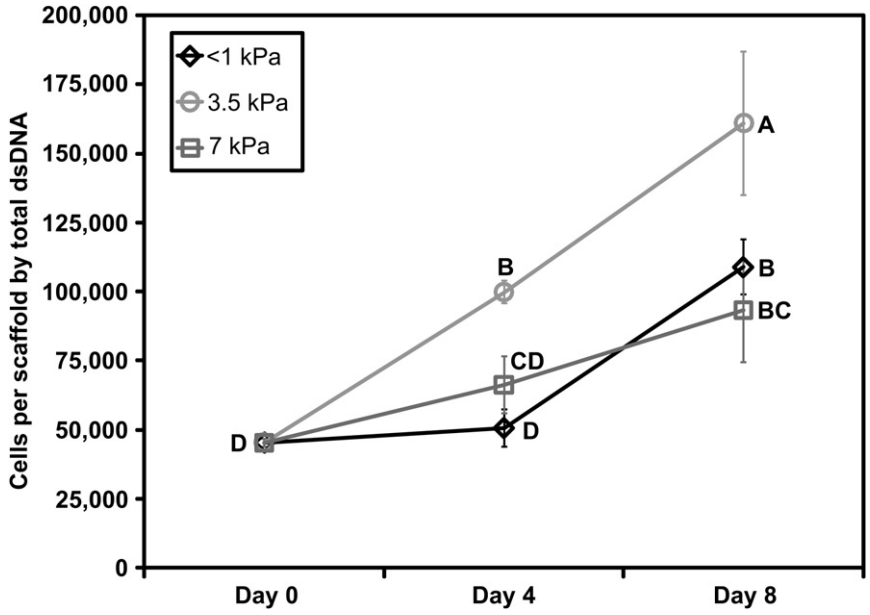

Fig. 5. Total cell number by PicoGreen assay for total dsDNA. By 8 d total cell number significantly increased for all stiffnesses as compared to 0 d, indicating proliferation. Significantly more cells were seen on 3.5 kPa MAC as compared to <1 and 7 kPa surfaces at 4 and 8 d. Different letters indicate significant differences by one-factor ANOVA ($p < 0.05$). Data are presented as mean ± SD, $n = 3$.

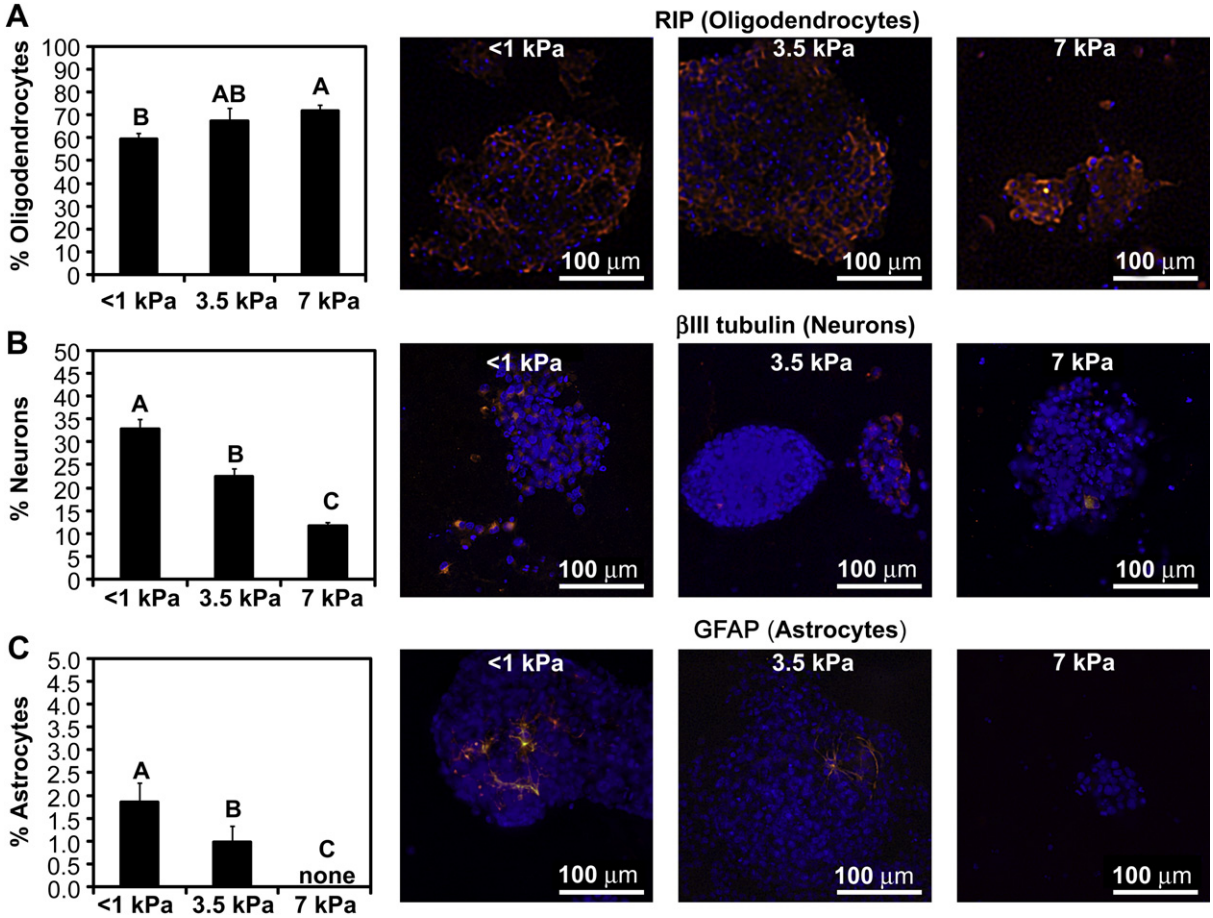

Fig. 6. Immunohistochemistry for differentiation into (A) oligodendrocytes, (B) neurons and (C) astrocytes after 8 d of culture. Stiffer MAC surfaces yielded a higher percentage of oligodendrocytes ($p < 0.001$). IHC images show that the majority of cells stain positive for RIP (oligodendrocytes) in colonies and on the surfaces of the gels. Softer surfaces favored both neuron and astrocyte differentiation ($p < 0.0001$). βIII positive cells (neurons) are observed in colonies and directly on <1 kPa surfaces. GFAP positive cells (astrocytes) occurred at low frequencies and were not seen on 7 kPa MAC. Different letters indicate significant differences by one-factor ANOVA ($p < 0.001$). Data are presented as mean ± SD, $n = 3$.

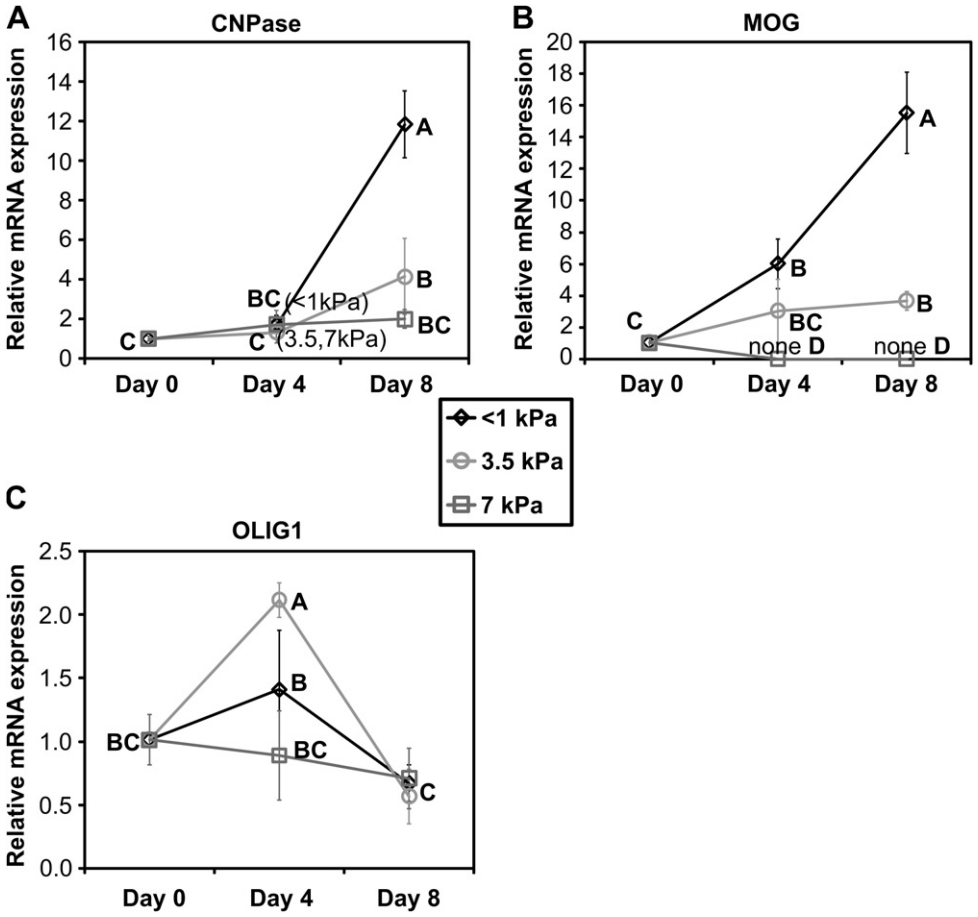

Fig. 7. Quantitative RT-PCR (fold change from day 0) for oligodendrocyte markers (A) 2′,3′-cyclic nucleotide 3′-phosphodiesterase (CNPase), (B) myelin oligodendrocyte glycoprotein (MOG) and (C) oligodendrocyte transcription factor 1 (OLIG1). CNPase mRNA expression was greatest on <1 kPa MAC ($p < 0.0001$) by 8 d. The mature marker MOG was only detectable on <1 kPa and 3.5 kPa surfaces and the greatest mRNA levels by 8 d on <1 kPa MAC ($p < 0.0001$). The transcriptional factor OLIG1 had increased expression only for 3.5 ka surfaces on day 4 ($p < 0.001$) and mRNA levels trended downward for all three hydrogels by 8 d. All data normalized to HPRT and GAPDH. Statistics by one-factor ANOVA, and means not connected by the same letter are significantly different ($p < 0.05$). Data presented as mean ± SD, $n = 4$.

(2 wt%). Transwell cultures demonstrated that UV crosslinked MAC did not adversely affect NSPC cell survival or proliferation (Fig. 3), validating its use in cell culture experiments. Following methacrylamide crosslinking, MAC hydrogels had over 50% of its repeat units functionalized with primary amines [30], facilitating covalent immobilization or ionic interactions of biomolecules. For example, we recently demonstrated that IFN-γ can be immobilized to the surface of MAC hydrogels through amide bond formation, stimulating the differentiation of adult rat SVZ-derived NSPCs into neurons [36]. Thus, MAC provides a system where the effects of both stiffness and biochemical factors can be investigated.

In this study, we show that adult SVZ-derived NSPC behavior varies markedly based on the mechanical properties of the culture substrate. Proliferation occurred on substrates with $E_Y < 1$–7 kPa (Fig. 5) and culture images (Fig. 4) reveal that this proliferation occurred in the form of colonies that increased in size throughout the 8 d culture period. Proliferation and colony formation ceased on MAC surfaces with $E_Y \geq 10$ kPa (Fig. 1). The greatest total cell numbers were seen on 3.5 kPa MAC surfaces which corresponded to the largest adherent colonies. Taken together, these results show that NSPC self-renewal is optimal between <1 and 7 kPa, indicating a connection to cell mechanotransductive pathways. The most likely candidate pathways would be linked to the mechanism by which cells anchor to substrates utilizing integrin-mediated focal adhesions (as reviewed in [37]). Laminin was included in all culture experiments to better mimic the adhesive environment found in the native NSPC niche as well as to facilitate activation of integrins and stimulate focal adhesion formation [29]. Studies of integrin-mediated mechanosensing have demonstrated that this mechanism begins with integrin activation which in turn directs integrin binding kinetics and clustering [38,39]. Tension has also been shown to initiate conformational changes to integrins, leading to higher activation states [40]. In light of these data, our data suggest that stiffness/compliance of the substrate may also alter spatial presentation of ECM binding ligands to their integrin receptors, leading to altered binding affinities and subsequent changes in transcriptional regulation of NSPC proliferation and differentiation; however, the consequences to downstream cell signaling pathways have not been elucidated.

Integrin activation is vital to cell function, however, activation of growth factor receptors and crosstalk with integrins is required to control both cell proliferation and differentiation [41]. The combination of these sensing modalities instructs the cellular response. On soft MAC surfaces (<1–7.5 kPa), integrin activation is likely an early event in the culture period (days 0–4), contributing to the proliferative response and initial formation of colonies. However, cell attachment likely transitions to a combination of integrins and other cell adhesion molecules (CAMs) as the cell colonies grow to exclude direct interactions of many of the cells in the colony with MAC surfaces. However, since cells in neurosphere colonies are

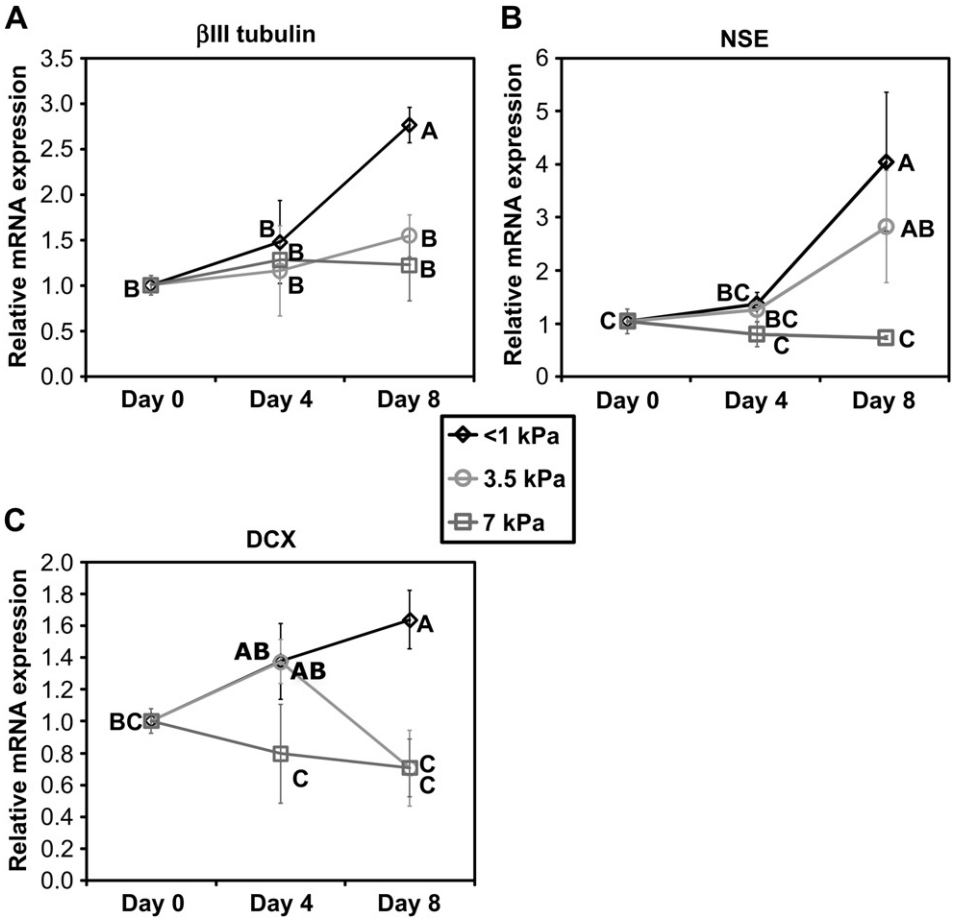

Fig. 8. Quantitative RT-PCR (fold change from day 0) for neuronal markers (A) βIII tubulin, (B) neuron specific enolase (NSE) and (C) doublecortin (DCX). βIII tubulin mRNA levels significantly increased on <1 kPa MAC by 8 d ($p < 0.0001$). NSE also significantly increased on <1 kPa surfaces ($p < 0.001$) and trended upward on 3.5 kPa surfaces after 8 d. The migrational marker DCX significantly increased on <1 kPa MAC over the culture period ($p < 0.001$). All data normalized to HPRT and GAPDH. Statistics by one-factor ANOVA, and means not connected by the same letter are significantly different ($p < 0.05$). Data presented as mean ± SD, $n = 4$.

known to actively secrete and assemble laminin [42,43], integrin activation likely remains a dominant cellular event throughout the culture period.

Results from IHC differentiation assays show that very soft surfaces best stimulate neuronal differentiation and that significantly more neurons were observed when the elastic modulus of the surface was decreased ($p < 0.0001$, Fig. 6B). These neuronal differentiation results are similar to the stiffness mediated response of adult hippocampal-derived NPSCs [20]. Close observation of IHC images showed that neurons existed on <1 kPa MAC surfaces in both colonies as well as directly on the surfaces, whereas neurons were nearly entirely observed in colonies on 3.5 and 7 kPa surfaces. These observations confirm that neurons prefer hydrogel surfaces with $E_Y < 1$ kPa. Quantitative RT-PCR confirmed that neuronal specific gene expression was highest on <1 kPa surfaces (Fig. 8). Compared to <1 kPa MAC, neuronal mRNA levels were lower on 3.5 kPa surfaces and even lower on 7 kPa surfaces where NSPCs maintained day 0 expressional levels for all neuronal markers assayed. This baseline mRNA expression was sufficient to result in 11.6 ± 0.8% of NSPCs differentiating into neurons by day 8 (Fig. 6B). The mRNA levels of the neuronal migrational marker DCX confirmed the increased cell migration that was observed on <1 kPa MAC by day 8 (Fig. 4) and suggests that a portion of these cells may be neurons undergoing chain migration, a process involving coordinated and radial cell movement that is unique to neurons differentiated from the SVZ [3,44].

Immunohistochemistry demonstrated that NSPCs differentiated primarily into oligodendrocytes on all substrates with 60% or more of all cells staining positive for RIP (Fig. 6B). This is consistent with previous reports which demonstrate that adult rat SVZ-derived NSPCs preferentially differentiate into oligodendrocytes in the presence of FBS [45,46]. Interestingly, IHC results demonstrated that stiffer surfaces favored oligodendrocyte differentiation whereas qRT-PCR results for CNPase and MOG expression demonstrated that the least stiff (<1 kPa) MAC surfaces favored oligodendrocyte differentiation (Fig. 7A and B). These results suggest that transcriptional levels of CNPase and MOG were elevated on a per cell basis on very soft MAC surfaces. CNPase transcriptional levels did not translate to protein levels (Fig. 6A) as RIP and CNPase immunoreactivity overlap [47], however, RIP immunohistochemistry is complex. Oligodendrocytes and Schwann cells are both RIP-immunoreactive and reactivity can be increased by the presence of other cell types and tissue injury [48]. The analysis of MOG gene expression suggests increased oligodendrocyte maturation and myelination on <1 kPa surfaces and may be a direct result of observed neuronal differentiation and maturation. High MOG mRNA levels are associated with maximal myelin deposition in the white matter where neuronal processes (axons) form and mature during development [49]. On <1 kPa MAC, high MOG mRNA levels corresponded to the greatest neuronal differentiation (Figs. 3B and 8). The lack of MOG expression and the least neuronal differentiation on 7 kPa MAC suggests that active myelin deposition and

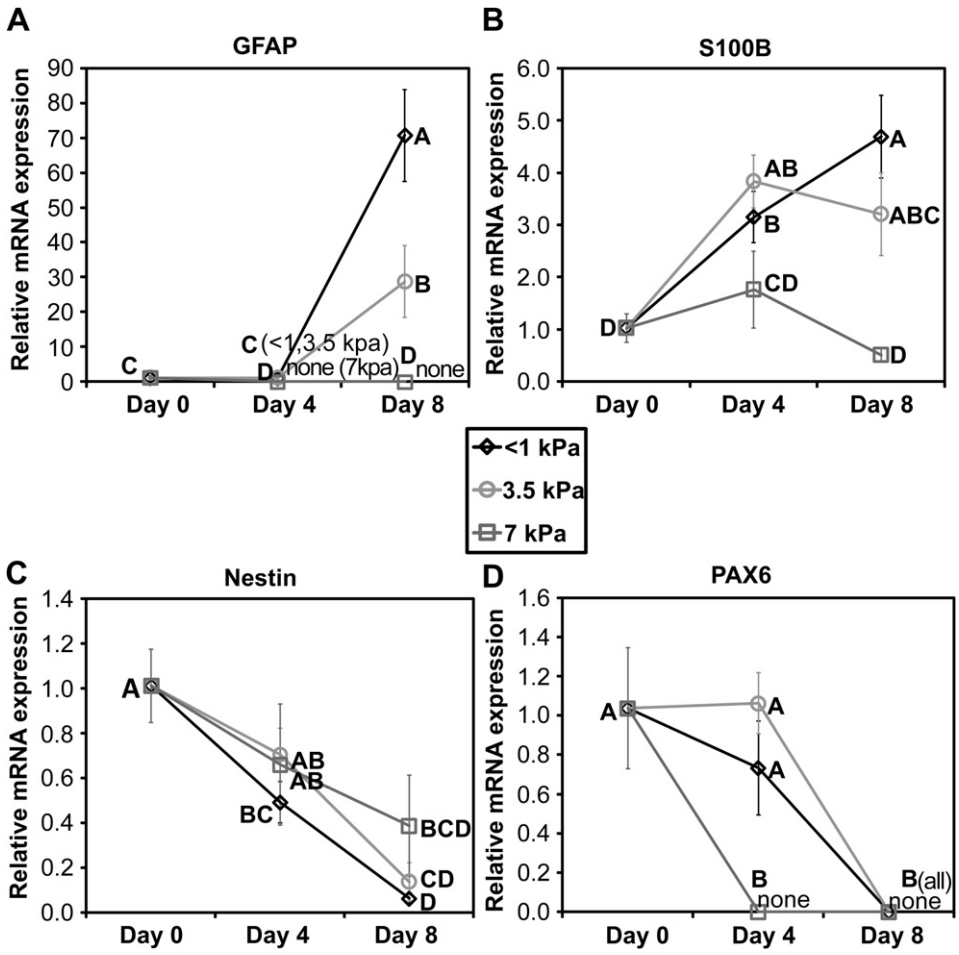

Fig. 9. Quantitative RT-PCR (fold change from day 0) for the astrocyte markers (A) glial fibrillary acidic protein (GFAP) and (B) calcium binding protein S100B as well as the progenitor markers (C) nestin and (D) Paired box gene 6 (PAX6). GFAP and S100B expression significantly increased on <1 and 3.5 kPa MAC after 8 d ($p < 0.05$). Nestin and PAX6 mRNA levels decreased on all surfaces over the culture period ($p < 0.05$). PAX6 expression was maintained from day 0 to day 4 before decreasing on <1 and 3.5 kPa MAC. All data normalized to HPRT and GAPDH. Statistics by one-factor ANOVA, and means not connected by the same letter are significantly different ($p < 0.05$). Data presented as mean ± SD, $n = 4$.

mature axon formation may not occur on stiffer surfaces (Fig. 7B). Our results demonstrate that a myelinating cell population is present for all stiffnesses of MAC, and that differences in maturation may exist. Quantifying the oligodendrocyte-specific proteins which are present when NSPCs are differentiated on MAC will allow a more thorough characterization of the RIP-immunoreactive cells that were observed in Fig. 6A. Additionally, qPCR data (Fig. 7) demonstrate that <1 kPa MAC generates a CNS-specific oligodendrocyte population with the highest expressional levels of CNPase, MOG and OLIG1. Previous work has demonstrated that CNPase, MOG and OLIG1 are expressed in both the CNS and PNS; however, mRNA levels of these genes are comparatively higher in the CNS [48,50,51].

In vivo the default differentiation pathway of SVZ stem cells is to neurons. Oligodendrocyte differentiation is not preferred, but can be stimulated after injury and when remyelination is required [52]. Here we demonstrate *in vitro* that substrate stiffness can also stimulate oligodendrocyte differentiation. This differentiation response could be clinically advantageous, offering cell based treatments for the repair of brain and spinal cord injuries as well as in addressing myelin disorders such as Multiple Sclerosis. Already implantation in spinal cord injured rats of oligodendrocyte progenitor cells (OPCs), induced from human embryonic stem cells, has demonstrated enhanced remyelination and partial restoration of locomotion [53]. Importantly, these significant results are being pursued in a clinical trial.

On MAC surfaces with moduli of <1–7 kPa, NSPC proliferation and colony formation were the preliminary cell responses that initiated cell differentiation. Substrate stiffness was influential in guiding colony formation as well as differentiation (Fig. 6). It is important to highlight that the influence of substrate stiffness on NSPC proliferation and differentiation is likely greatest at the beginning of the culture period, when most cells directly interact with the surface and before large colonies have formed. The stiffness of the matrix orchestrates the selection of certain progenitor populations, encouraging their proliferation and eventual differentiation. During later time points the stiffness of the substrate was shown to influence the presence of differentiated neurons on the surface, away from colonies and only on <1 kPa surfaces (Fig. 6B). Substrates with E_Y between <1 and 7 primarily stimulated the proliferation of oligodendrocytes and neuron progenitors which resided in the growing colonies. The majority of the observed proliferation can likely be attributed to progenitors, since neurosphere culture in proliferation media has demonstrated that uncommitted neural stem cells make up less than 1% of the total population [54]. During the course of the 8 d culture period, this pool of progenitors decreased overall, as shown by down regulation of nestin mRNA expression (Fig. 9A). The presence of nestin positive cells was confirmed with IHC at day 8, yet nestin positive cells were present at low frequencies and only in colonies (data not shown). Colonies maintained expression of the transcriptional factor and neuronal progenitor specific marker PAX6

on <1 and 3.5 kPa surfaces for 4 d before turning off expression, confirming neuronal maturation. PAX6 has been previously tied to neural stem/early progenitor cells that first differentiate into GFAP positive radial glia followed by neurons [34,35]. Interestingly, we observed that the down regulation of PAX6 mRNA levels (Fig. 9C) corresponded with the up-regulation of both S100B and GFAP mRNA levels (Fig. 9A) as well as the appearance of GFAP-positive immunostained cells (Fig. 6C).

MAC offers a biomaterial based culture system which can be utilized to study and tune microenvironmental cues in order to more precisely guide stem cell behavior. Future work will focus on 3D responses to niche cues both *in vitro* and *in vivo*, which is possible with photopolymerizable MAC. Similar methodologies have been utilized for encapsulating live cells in methacrylate poly(ethylene glycol) hydrogels including studies with embryonic NSPCs [55]. A tunable photocrosslinkable material such as MAC facilitates the study of the combined actions of substrate stiffness, adhesive ligands, growth factor signals and co-culture with other cell types. Such a system may allow spatial control of cell differentiation, protein synthesis and the creation of tissue structures to replace diseased or damaged tissues in the nervous system.

5. Conclusions

Adult stem cells reside in unique niches, providing the cues necessary to guide proliferation and differentiation. This work demonstrates that photopolymerizable MAC can be utilized to study the contribution of substrate stiffness to NSPC behavior while also providing cells with similar soluble and adhesive cues to those found in the native NSPC niche. We have demonstrated that an optimal stiffness exists for both proliferation (3.5 kPa) as well as differentiation to neurons (<1 kPa). Oligodendrocyte and astrocyte differentiation are closely tied to proliferation and colony formation as well as the presence of neurons. The results of this study are important for the creation of biomaterials targeted towards CNS regeneration as well for understanding the basic principles influencing stem cell behavior and function.

Acknowledgments

We are grateful to partial funding from the Natural Sciences and Engineering Research Council of Canada (NSERC Discovery grant to MSS), Ontario Ministry of Research and Innovation postdoctoral fellowship (NDL) and the Advanced Food and Materials Network (AFM-Net to MSS). The authors thank Dr. Tasneem Zahir for stimulating discussions and assistance with neural stem cell assays, Dr. Ying Fang Chen for assistance with cell culture, Dr. Laura Yu for help with the synthesis of MAC, Ryan Wylie for assistance creating and purifying FAM–laminin and Xiao Yang for his assistance with SEM. We also would like to thank Dr. Derek van der Kooy for allowing us to perform qRT-PCR analysis in his laboratory.

Appendix

Figures with essential colour discrimination. Fig. 6 is in this article is difficult to interpret in black and white. The full colour version can be found in the on-line version, at doi:10.1016/j.biomaterials.2009.09.002.

References

[1] Morrison SJ, Shah NM, Anderson DJ. Regulatory mechanisms in stem cell biology. Cell 1997;88:287–98.
[2] Reynolds BA, Weiss S. Generation of neurons and astrocytes from isolated cells of the adult mammalian central nervous system. Science 1992;255:1707–10.
[3] Gage FH. Mammalian neural stem cells. Science 2000;287:1433–8.
[4] Temple S. The development of neural stem cells. Nature 2001;414:112–7.
[5] Ayuso-Sacido A, Roy NS, Schwartz TH, Greenfield JP, Boockvar JA. Long-term expansion of adult human brain subventricular zone precursors. Neurosurgery 2008;62:223–9. discussion 229–31.
[6] Shetty AK, Turner DA. In vitro survival and differentiation of neurons derived from epidermal growth factor-responsive postnatal hippocampal stem cells: inducing effects of brain-derived neurotrophic factor. J Neurobiol 1998;35:395–425.
[7] Whittemore SR, Morassutti DJ, Walters WM, Liu RH, Magnuson DS. Mitogen and substrate differentially affect the lineage restriction of adult rat subventricular zone neural precursor cell populations. Exp Cell Res 1999;252:75–95.
[8] Benoit BO, Savarese T, Joly M, Engstrom CM, Pang L, Reilly J, et al. Neurotrophin channeling of neural progenitor cell differentiation. J Neurobiol 2001;46:265–80.
[9] Gomes WA, Mehler MF, Kessler JA. Transgenic overexpression of BMP4 increases astroglial and decreases oligodendroglial lineage commitment. Dev Biol 2003;255:164–77.
[10] Engler A, Bacakova L, Newman C, Hategan A, Griffin M, Discher D. Substrate compliance versus ligand density in cell on gel responses. Biophys J 2004;86:617–28.
[11] Halliday NL, Tomasek JJ. Mechanical properties of the extracellular matrix influence fibronectin fibril assembly in vitro. Exp Cell Res 1995;217:109–17.
[12] Pelham Jr RJ, Wang Y. Cell locomotion and focal adhesions are regulated by substrate flexibility. Proc Natl Acad Sci U S A 1997;94:13661–5.
[13] Balgude AP, Yu X, Szymanski A, Bellamkonda RV. Agarose gel stiffness determines rate of DRG neurite extension in 3D cultures. Biomaterials 2001;22:1077–84.
[14] Cukierman E, Pankov R, Stevens DR, Yamada KM. Taking cell–matrix adhesions to the third dimension. Science 2001;294:1708–12.
[15] Deroanne CF, Lapiere CM, Nusgens BV. In vitro tubulogenesis of endothelial cells by relaxation of the coupling extracellular matrix-cytoskeleton. Cardiovasc Res 2001;49:647–58.
[16] Flanagan LA, Ju YE, Marg B, Osterfield M, Janmey PA. Neurite branching on deformable substrates. Neuroreport 2002;13:2411–5.
[17] Engler AJ, Griffin MA, Sen S, Bonnemann CG, Sweeney HL, Discher DE. Myotubes differentiate optimally on substrates with tissue-like stiffness: pathological implications for soft or stiff microenvironments. J Cell Biol 2004;166:877–87.
[18] Engler AJ, Sen S, Sweeney HL, Discher DE. Matrix elasticity directs stem cell lineage specification. Cell 2006;126:677–89.
[19] Georges PC, Miller WJ, Meaney DF, Sawyer ES, Janmey PA. Matrices with compliance comparable to that of brain tissue select neuronal over glial growth in mixed cortical cultures. Biophys J 2006;90:3012–8.
[20] Saha K, Keung AJ, Irwin EF, Li Y, Little L, Schaffer DV, et al. Substrate modulus directs neural stem cell behavior. Biophys J 2008;95:4426–38.
[21] Taylor Z, Miller K. Reassessment of brain elasticity for analysis of biomechanisms of hydrocephalus. J Biomech 2004;37:1263–9.
[22] Gefen A, Margulies SS. Are in vivo and in situ brain tissues mechanically similar? J Biomech 2004;37:1339–52.
[23] Collinsworth AM, Zhang S, Kraus WE, Truskey GA. Apparent elastic modulus and hysteresis of skeletal muscle cells throughout differentiation. Am J Physiol Cell Physiol 2002;283:C1219–27.
[24] Athanasiou KA, Rosenwasser MP, Buckwalter JA, Malinin TI, Mow VC. Interspecies comparisons of in situ intrinsic mechanical properties of distal femoral cartilage. J Orthop Res 1991;9:330–40.
[25] Katsamanis F, Raftopoulos DD. Determination of mechanical properties of human femoral cortical bone by the Hopkinson bar stress technique. J Biomech 1990;23:1173–84.
[26] Yu Q, Zhou J, Fung YC. Neutral axis location in bending and Young's modulus of different layers of arterial wall. Am J Physiol 1993;265:H52–60.
[27] Lu YB, Franze K, Seifert G, Steinhauser C, Kirchhoff F, Wolburg H, et al. Viscoelastic properties of individual glial cells and neurons in the CNS. Proc Natl Acad Sci U S A 2006;103:17759–64.
[28] Morshead CM, Benveniste P, Iscove NN, van der Kooy D. Hematopoietic competence is a rare property of neural stem cells that may depend on genetic and epigenetic alterations. Nat Med 2002;8:268–73.
[29] Campos LS. Beta1 integrins and neural stem cells: making sense of the extracellular environment. Bioessays 2005;27:698–707.
[30] Yu LM, Kazazian K, Shoichet MS. Peptide surface modification of methacrylamide chitosan for neural tissue engineering applications. J Biomed Mater Res A 2007;82:243–55.
[31] Leipzig ND, Athanasiou KA. Unconfined creep compression of chondrocytes. J Biomech 2005;38:77–85.
[32] Zahir T, Nomura H, Guo XD, Kim H, Tator C, Morshead C, et al. Bioengineering neural stem/progenitor cell-coated tubes for spinal cord injury repair. Cell Transplant 2008;17:245–54.
[33] Pfaffl MW, Tichopad A, Prgomet C, Neuvians TP. Determination of stable housekeeping genes, differentially regulated target genes and sample integrity: BestKeeper – excel-based tool using pair-wise correlations. Biotechnol Lett 2004;26:509–15.
[34] Kohwi M, Osumi N, Rubenstein JL, Alvarez-Buylla A. Pax6 is required for making specific subpopulations of granule and periglomerular neurons in the olfactory bulb. J Neurosci 2005;25:6997–7003.
[35] Osumi N, Shinohara H, Numayama-Tsuruta K, Maekawa M. Concise review: Pax6 transcription factor contributes to both embryonic and

adult neurogenesis as a multifunctional regulator. Stem Cells 2008;26:1663–72.
[36] Leipzig ND, Xu C, Zahir T, Shoichet MS. Functional immobilization of interferon-gamma induces neuronal differentiation of neural stem cells. J Biomed Mater Res: Part A, in press.
[37] Puklin-Faucher E, Sheetz MP. The mechanical integrin cycle. J Cell Sci 2009;122:179–86.
[38] Kim M, Carman CV, Yang W, Salas A, Springer TA. The primacy of affinity over clustering in regulation of adhesiveness of the integrin {alpha}L{beta}2. J Cell Biol 2004;167:1241–53.
[39] Cluzel C, Saltel F, Lussi J, Paulhe F, Imhof BA, Wehrle-Haller B. The mechanisms and dynamics of (alpha)v(beta)3 integrin clustering in living cells. J Cell Biol 2005;171:383–92.
[40] Friedland JC, Lee MH, Boettiger D. Mechanically activated integrin switch controls alpha5beta1 function. Science 2009;323:642–4.
[41] Streuli CH. Integrins and cell-fate determination. J Cell Sci 2009;122:171–7.
[42] Campos LS, Leone DP, Relvas JB, Brakebusch C, Fassler R, Suter U, et al. Beta1 integrins activate a MAPK signalling pathway in neural stem cells that contributes to their maintenance. Development 2004;131:3433–44.
[43] Milner R. A novel three-dimensional system to study interactions between endothelial cells and neural cells of the developing central nervous system. BMC Neurosci 2007;8:3.
[44] Lois C, Garcia-Verdugo JM, Alvarez-Buylla A. Chain migration of neuronal precursors. Science 1996;271:978–81.
[45] Aizawa Y, Leipzig N, Zahir T, Shoichet M. The effect of immobilized platelet derived growth factor AA on neural stem/progenitor cell differentiation on cell-adhesive hydrogels. Biomaterials 2008;29:4676–83.
[46] Nomura H, Zahir T, Kim H, Katayama Y, Kulbatski I, Morshead CM, et al. Extramedullary chitosan channels promote survival of transplanted neural stem and progenitor cells and create a tissue bridge after complete spinal cord transection. Tissue Eng Part A 2008;14:649–65.
[47] Watanabe M, Sakurai Y, Ichinose T, Aikawa Y, Kotani M, Itoh K. Monoclonal antibody Rip specifically recognizes 2′,3′-cyclic nucleotide 3′-phosphodiesterase in oligodendrocytes. J Neurosci Res 2006;84:525–33.
[48] Toma JS, McPhail LT, Ramer MS. Differential RIP antigen (CNPase) expression in peripheral ensheathing glia. Brain Res 2007;1137:1–10.
[49] Pham-Dinh D, Mattei MG, Nussbaum JL, Roussel G, Pontarotti P, Roeckel N, et al. Myelin/oligodendrocyte glycoprotein is a member of a subset of the immunoglobulin superfamily encoded within the major histocompatibility complex. Proc Natl Acad Sci U S A 1993;90:7990–4.
[50] Pagany M, Jagodic M, Schubart A, Pham-Dinh D, Bachelin C, Baron van Evercooren A, et al. Myelin oligodendrocyte glycoprotein is expressed in the peripheral nervous system of rodents and primates. Neurosci Lett 2003;350:165–8.
[51] Li H, Lu Y, Smith HK, Richardson WD. Olig1 and Sox10 interact synergistically to drive myelin basic protein transcription in oligodendrocytes. J Neurosci 2007;27:14375–82.
[52] Menn B, Garcia-Verdugo JM, Yaschine C, Gonzalez-Perez O, Rowitch D, Alvarez-Buylla A. Origin of oligodendrocytes in the subventricular zone of the adult brain. J Neurosci 2006;26:7907–18.
[53] Keirstead HS, Nistor G, Bernal G, Totoiu M, Cloutier F, Sharp K, et al. Human embryonic stem cell-derived oligodendrocyte progenitor cell transplants remyelinate and restore locomotion after spinal cord injury. J Neurosci 2005;25:4694–705.
[54] Reynolds BA, Rietze RL. Neural stem cells and neurospheres–re-evaluating the relationship. Nat Methods 2005;2:333–6.
[55] Mahoney MJ, Anseth KS. Three-dimensional growth and function of neural tissue in degradable polyethylene glycol hydrogels. Biomaterials 2006;27:2265–74.